Surface electronic structure of γ-uranium

You Gong Hao

Department of Physics, West Virginia University, Morgantown, West Virginia 26506-6315

Olle Eriksson

Center for Materials Science, Los Alamos National Laboratory, Los Alamos, New Mexico 87545

Gayanath W. Fernando*

Physics Department, Brookhaven National Laboratory, Upton, New York 11973

Bernard R. Cooper

Department of Physics, West Virginia University, Morgantown, West Virginia 26506-6315
and Center for Materials Science, Los Alamos National Laboratory, Los Alamos, New Mexico 87545

It is interesting to study the surface electronic structure of uranium in the context of f-electron localization as the $5f$ shell is filled. Accordingly, we have used the film-linearized-muffin-tin-orbital method to calculate the surface electronic structure of γ-uranium with body-centered-cubic structure. This all-electron self-consistent fully relativistic calculation has been done for a five-layer slab with (100) surface using two lattice constants (differing by about 1%) corresponding to different experimental information. Our calculated work functions of 3.60 and 3.82 eV for the two lattice constants both provide excellent agreement with the experimental results, which range from 3.63 to 3.90 eV. The calculated density of states and the charge distribution show stronger hybridization of $5f$ with $6d$ electrons than that of δ-plutonium. Our calculations indicate that the surface enhancement of $5f$ localization (i.e., relative to the bulk behavior) is much stronger for uranium than for plutonium. This increase of localization at the surface may have important consequences for surface reconstruction, chemisorption, and other surface behavior.

I. INTRODUCTION

It is interesting to study the surface behavior of the early actinides (thorium through plutonium) in the context of f-electron localization as the $5f$ shell is filled.[1,2] For the bulk electronic behavior, as the proportion of $5f$ to $6d$ and $7s$ electrons increases, the itinerant behavior of the $5f$ electrons gradually disappears (with a more drastic change to localization between Pu and Am). Since the surface f electrons tend to be somewhat more localized than those in the interior (because of decreased opportunity for overlap), the degree of localized f-electron behavior will be more conspicuous at the surface for any of the light actinides. Furthermore, several experimentally accessible surface properties such as the work function[3] and chemical reactivity are quite sensitive monitors of the degree of f-electron localization. Uranium, located in the middle of the early part of the series, has only three $5f$ electrons in its atomic configuration ($5f^3 6d^1 7s^2$) instead of the six $5f$ electrons in plutonium ($5f^6 7s^2$), and the proportion of outer-shell s and d electrons is also larger in uranium than in plutonium. Therefore, a study of the electronic structure of uranium provides important information about the changeover from itinerant to localized $5f$-electron behavior. It is therefore illuminating to calculate the predicted surface behavior for uranium and to compare this behavior to that which we calculated for plutonium.[3] Moreover, since uranium metal is highly reactive with almost all nonmetallic chemical agents, especially with hydrogen, oxygen, and water, and with many metallic elements as well,[4] a study of the surface electronic structure of uranium is of great potential practical importance.

II. METHOD AND GEOMETRY

The method employed in this study is our self-consistent film-linearized-muffin-tin-orbital (FLMTO) method.[5] The method has been proven by a number of calculations of $3d$, $4d$, and $5f$ metals[3,6-8] to be an efficient and accurate way to provide high-quality results. Since it has been described in detail in our previous work,[3,6-8] we give only a brief description here.

The basis functions used are a combination of the standard muffin-tin orbitals (MTO's) (Ref. 9) and plane-wave orbitals (PWO's).[5,7] The MTO's inside the sphere consist of a linear combination of the solution of the radial Dirac equation and its energy derivative for the spherically averaged actual potential at each iteration. We do not use the atomic-sphere approximation;[10] the full potential is used everywhere except inside the muffin-tin spheres where the non-muffin-tin (NMT) potential is approximated by the extended interstitial NMT potential. In the interstitial region, the MTO is a Hänkel function, while in the vacuum it is modified to be a linear combination of the solution of the one-dimensional Schrödinger equation

and its energy derivative for the planar averaged vacuum potential. The PWO's as independent basis functions, behave like two-dimensional plane waves in the direction parallel to the slab surface. Along the direction perpendicular to the surface, they either have a real exponential behavior or a plane-wave-like behavior, depending on the energy parameter and parallel reciprocal-lattice vector in the interstitial region. Like the MTO's, the PWO's are augmented inside the muffin-tin spheres. In the vacuum they have the form of linear combinations of solutions of the one-dimensional Schrödinger equation for the vacuum potential and their energy derivatives. All these functions are continuous and have continuous first derivatives everywhere. Both valence and core electrons are treated self-consistently. The energy parameters for each orbital in the spheres and for the vacuum and interstitial regions are calculated self-consistently, which leaves the lattice constant, atomic number, and valence-electron number as the only input. The exchange-correlation potential is calculated within the local-spin-density approximation using the Vosko-Wilk-Nusair parametrization.[11] The iterative calculations were carried out until the difference in input and output potential was of the order of a few mRy at all locations.

There are three forms of uranium structures that occur as the temperature changes[12] (orthorhombic α-U up to 600° C, tetragonal β-U up to 760 °C, and bcc γ-U above 760° C). In the high-temperature γ phase, the structure has been found[4] to be body-centered cubic. A lattice constant of 3.48 Å was found at high temperature. This value is then extrapolated to a room-temperature lattice constant of[4] 3.43 Å. The lattice constant of γ-uranium at room temperature has also been studied by means of
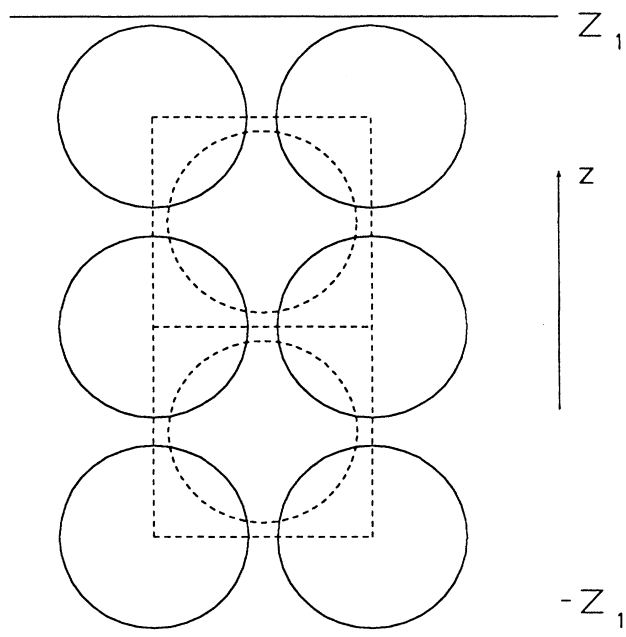
impurity-stabilized samples, from which a pure γ-uranium lattice constant at room temperature is derived to be[4] 3.467 Å. With this information in mind, we have performed calculations for a (100)-oriented five-layer slab of bcc uranium as shown in Fig. 1, with lattice constants of both 3.43 and 3.467 Å. In both calculations, we adjusted the radius of the muffin-tin sphere to make the spheres touch.

For both lattice constants a ten-point set of special k points in the irreducible wedge of the Brillouin zone of the two-dimensional square mesh has been used in the calculations.[13] The two choices of lattice constant yield very similar densities of states (DOS) and charge-density distributions, and give work-function values of 3.82 and 3.60 eV for the smaller and larger lattice constants, respectively. Both these values provide excellent agreement with the most recent experimental values,[14,15] which range from 3.63 to 3.90 eV.

III. RESULTS OF THE CALCULATION

A. Electronic structure

Since the calculation for the lattice constant of 3.43 Å gives a density of states and charge-density distribution very similar to those for the lattice constant of 3.467 Å, we show only the density of states and the charge-density distribution contour map for the latter. By employing the Lorentzian broadening smoothing technique[16] (with the smoothing factor $\lambda = 0.03$ eV) we plot the density of states from the calculated discrete energy eigenvalues. In the sphere-projected density of states shown in Fig. 2, the spin-orbit splitting is 1.1 eV, as expected, slightly less than the 1.3 eV splitting for plutonium.[3] This small increase from uranium to plutonium is consistent with the charge being concentrated closer to the nucleus as the actinide contraction occurs.

The density-of-states behavior for uranium corresponds to much broader f-band widths than for plutonium. Indeed, in this calculation, the density of states for the center (bulklike) sphere does not show a distinctly two-peak structure. This is very different from what we have found in the plutonium calculation,[3] in which we found two peaks, mainly originating from $\frac{5}{2}$ and $\frac{7}{2}$ states, respectively, with the $\frac{5}{2}$ band and the $\frac{7}{2}$ band fairly well separated. In the uranium calculation of Fig. 2 however, the $\frac{5}{2}$ band and the $\frac{7}{2}$ band are very much overlapped, especially at energies lower than the Fermi level. Moreover, the $\frac{5}{2}$ band and the $\frac{7}{2}$ band are both much wider than those of plutonium. The shorter distance between two nearest atoms in γ-uranium compared to the distance in δ-plutonium makes the direct overlap of $5f$ orbitals stronger, and this leads to the f-band width for uranium being larger than that for plutonium. However, although the surface density-of-states peaks ($\frac{5}{2}$ and $\frac{7}{2}$) for U are broader than the corresponding DOS peaks for Pu, the narrowing relative to bulk behavior is greater in U. Thus, the contrast between U and Pu in itinerancy of f-electron behavior is less pronounced on the surface than in the bulk.

In addition to the direct overlap between the f orbitals,

FIG. 1. Geometry of the five-layer γ-uranium slab. The z direction is normal to the surfaces at $\pm Z_1$. Solid and dashed circles show uranium atoms at the body-centered positions in alternating layers looking inward.

TABLE I. Integrated charge distribution of bcc γ-uranium for lattice constants of 3.43 and 3.467 Å shown for the center, subsurface, and surface atomic spheres (orbitally projected) and the interstitial region of the five-layer slab.

Integrated orbital-projected and interstitial charge distribution (e^-) $(a = 3.43$ Å$)$			
	s	p	d	f
Center	0.265	0.138	1.779	2.551
Subsurface	0.287	0.108	1.805	2.536
Surface	0.223	0.095	1.218	2.586

Interstitial charge = 7.304 per five-atom unit cell

$(a = 3.467$ Å$)$			
	s	p	d	f
Center	0.280	0.143	1.790	2.512
Subsurface	0.304	0.112	1.823	2.489
Surface	0.237	0.098	1.225	2.580

Interstitial charge = 7.293 per five-atom unit cell

the stronger hybridization between f and s, p and d orbitals, especially between f and d orbitals, contributes to the broadening of the f peaks. This can be seen from the charge distribution for the orbitals as shown in Table I, when considered together with the locations of the orbitals in the density-of-states plots shown in Fig. 3. In the orbital-projected charge distribution for the spin-orbit-split case with $a = 3.467$ Å shown in Table I, we note that the d-orbital charge for the center atom is 38% of the total charge, which is almost double the d-orbital charge of 19% of the total charge for the center atom in the plutonium calculation.[3] In Fig. 3 we plot the orbital-projected density of states for the center, subsurface, and surface spheres. In order to make the behavior of the s, p, and d states more visible, we have enlarged the density of those states by a factor of 5 in the plot. We see that the wide d-band density extends from -4 eV to well above the Fermi level with the low-energy tail of the f-

FIG. 2. Sphere-projected density of states for the $a = 3.467$ Å slab calculation. Fermi energy is at zero.
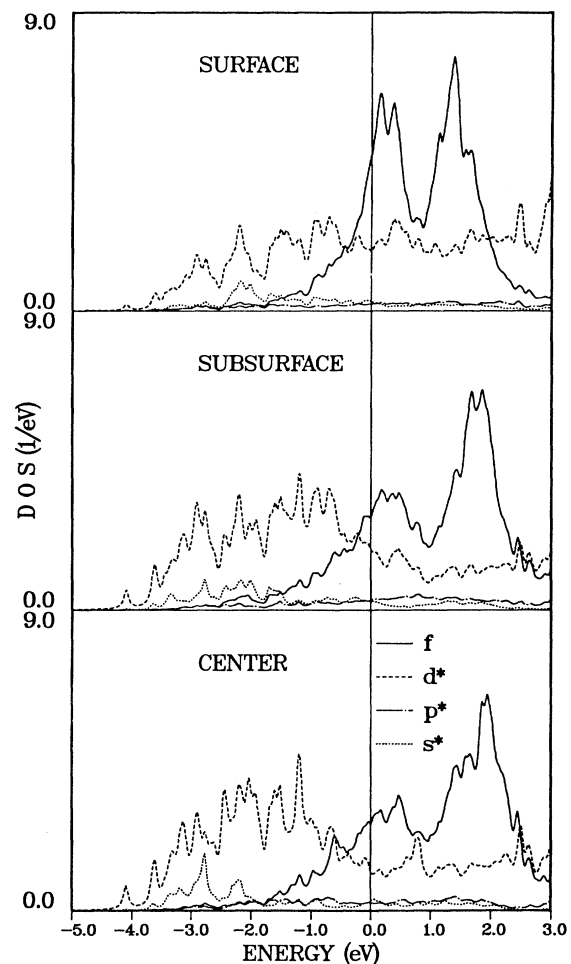
FIG. 3. Orbital-projected density of states for the center, subsurface, and surface spheres, respectively. Note that the density of s^*, p^*, and d^* states has been enlarged by a factor of 5. In the figure, the dotted lines are for s electrons, the dot-dashed lines are for p electrons, the dashed lines are for d electrons, and the solid lines are for f electrons. The Fermi energy is at zero.

band density lying on top of it. The d-band density is quite significant compared to that of the f bands, especially in the center and subsurface spheres. In comparison to the d bands, the smaller s- and p-band densities are basically featureless over their broad extent, as is expected for plane-wave-like behavior. In addition to the approximately 0.4 electrons of s/p density in each sphere, the substantial interstitial charge density shown in Table I (1.4 electrons per atom) probably also is largely derived from the s atomic states. The behavior shown in Fig. 3, with large d-band density overlapping diminished f-band density in the lower part of the energy range gives more opportunity for d-f mixing, and thus we find significant hybridization between d and f orbitals. The d-electron density-of-states behavior of Fig. 3, with d-DOS growth at energies lower than the main part of the f DOS is consistent with the antiresonance character that would be expected in the Fano-Anderson model.[17]

B. Charge-distribution contour map

The charge-distribution contour maps for slices perpendicular to the slab surface with orientations parallel to [$\bar{1}$10] and [100] planes are given abutted to each other in Fig. 4. In addition to the basically spherical nature of the charge distribution around each atomic site, we notice that the charge density shows an increase between the spheres as compared to the distribution for plutonium. This directionality of charge gives evidence of covalent bonding.

$[\bar{1}10]$ $[100]$
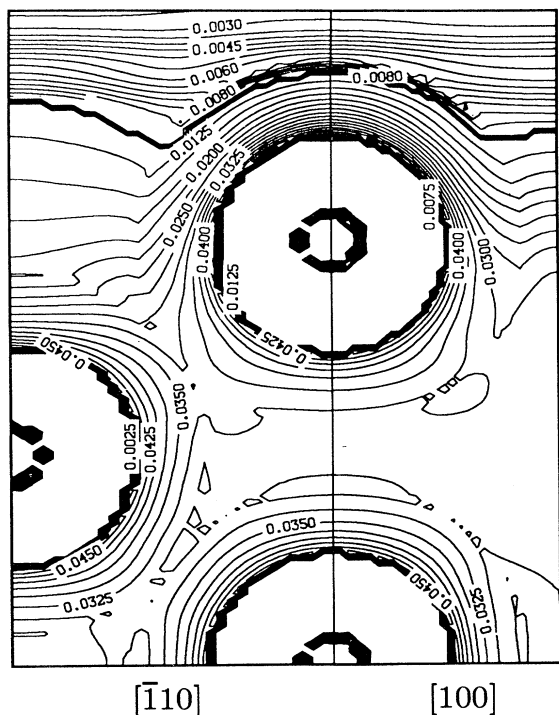
FIG. 4. Charge-density-distribution contour maps for slices perpendicular to the slab surface with orientations parallel to [$\bar{1}$10] and [100] planes abutted to each other. The charge density is in units of electron/(a.u.)^3 (spacing between contours shown on the figure).

TABLE II. Integrated interstitial/vacuum charge distribution and work function for bcc γ-uranium with lattice constants of 3.43 and 3.467 Å.

	Interstitial/Vacuum charge	Work function
3.43 Å	7.304/0.243 (e^-)	3.82 (eV)
3.467 Å	7.293/0.245 (e^-)	3.60 (eV)

C. Work functions and charge distribution

Based on our previous experience with noble and transition metal systems,[7,8] we expect properly converged FLMTO calculations of the work function to be reliable within a few tenths of an eV or less. The most recent experimental work for the uranium work function gives[14] 3.63 eV for uranium deposited on polycrystalline tungsten and[15] 3.73, 3.90, and 3.67 eV for uranium deposited on (100), (110), and (113) surfaces of single-crystal tungsten, respectively, while in the present calculations we found that the work function for (100) γ-uranium is 3.82 eV for a lattice constant of 3.43 Å and 3.60 eV for a lattice constant of 3.467 Å. Thus, the agreement with experiment is excellent and appears to be of the same quality as that expected for noble and transition metals. The small difference between the calculated work functions for the two lattice constants apparently arises from the circumstance that the smaller lattice constants cause the electrons to move slightly more out of the muffin-tin spheres and to spread out further into the interstitial and vacuum regions. This slightly increases the surface dipole moment, which then increases the work function (see Table II).

IV. CONCLUSIONS

The relationship of surface electronic behavior to the changeover of the $5f$ electronic behavior from that of an itinerant transition-metal-like system to that of a localized lanthanidelike system in the early part of the actinides is our main concern in this investigation. In this regard, the most interesting result is the behavior shown in Fig. 2, where we found that the band width at the surface is much narrower than that in the bulk; this indicates that the surface enhancement of $5f$ localization relative to that in the bulk is much stronger for uranium than for plutonium.[3] While the overall band widths for uranium are wider than that for plutonium, the narrowing of the surface band width is larger for uranium than for plutonium. This indicates that the surface electronic properties of uranium are significantly different from those in the bulk. Plutonium has probably the most complicated crystal-structure behavior of any element, with some six different structures occurring before melting; and this behavior has been discussed[18] as being related to the f-electron behavior being at the borderline between itinerant and localized behavior. The increased f localization at the surface of uranium thus makes surface uranium more "plutoniumlike." This may imply a tendency toward possibly complicated surface reconstruction. This could be important, especially for chemisorption at the uranium surface. For uranium, because of its more transition-metal-like behavior, there might be a sur-

face contraction favorable to increased bonding,[19] while for plutonium there might be a surface expansion more favorable to the polarization effects (and even possibly a surface magnetic transition).

*Present address: Department of Physics, University of Connecticut, Storrs, CT 06268.

[1] *The Actinides Electronic Structure and Related Properties*, edited by A. J. Freeman and J. B. Darby, Jr. (Academic, New York, 1974).

[2] *Handbook on the Physics and Chemistry of the Actinides*, edited by A. J. Freeman and G. H. Lander (North-Holland, Amsterdam, 1985).

[3] Y. G. Hao, O. Eriksson, G. W. Fernando, and B. R. Cooper, Phys. Rev. B **43**, 9467 (1991).

[4] *The Chemistry of Uranium*, edited by J. Katz and E. Rabinowitch (McGraw-Hill, New York, 1951).

[5] H. Krakauer and B. R. Cooper, Phys. Rev. B **16**, 605 (1977).

[6] C. Q. Ma, M. V. Ramana, B. R. Cooper, and H. Krakauer, Phys. Rev. B **34**, 3854 (1986).

[7] G. W. Fernando, B. R. Cooper, M. V. Ramana, H. Krakauer, and C. Q. Ma, Phys. Rev. Lett. **56**, 2299 (1986).

[8] G. W. Fernando and B. R. Cooper, Phys. Rev. B **38**, 3016 (1988).

[9] O. K. Anderson, Phys. Rev. B **12**, 3060 (1975).

[10] H. L. Skriver, *The LMTO Method* (Springer-Verlag, Berlin, 1984).

[11] S. H. Vosko, L. Wilk, and N. Nusair, Can. J. Phys. **58**, 1200 (1980).

[12] *Structural Inorganic Chemistry*, 5th ed., edited by A. F. Wells (Oxford Science, Oxford, 1984), p. 1284.

[13] S. L. Cunningham, Phys. Rev. B **10**, 4988 (1974).

[14] B. J. Hopkins and A. J. Sargood, Suppl. Nuovo Cimento **5**, 459 (1967).

[15] C. Lea and C. H. B. Mee, J. Appl. Phys. **39**, 5890 (1968).

[16] B. Lindgen and D. E. Ellis, Phys. Rev. B **26**, 636 (1982).

[17] See pp. 272–285 in G. D. Mahan, *Many-Particle Physics*, 2nd ed. (Plenum, New York, 1990).

[18] J. L. Smith, Z. Fisk, and S. S. Hecker, Physica **130B**, 151 (1985).

[19] N. Takeuchi, C. T. Chan, and K. M. Ho, Phys. Rev. Lett. **63**, 1273 (1989).